La Metallurgia Italiana
International Journal of the Italian Association for Metallurgy

Numerical simulation of laser powder bed fusion processes

edited by: M. B. Abrami, C. Ransenigo, M.Tocci, A. Pola, M. Obeidi, D. Brabazon

The need to create increasingly high-performance components using additive manufacturing (AM) technologies appears now extremely pressing. In this context, the recently developed numerical simulation software of AM processes can represent a powerful tool for predicting the influence of the different parameters on final performances. As for any process simulation, the reliability of the results depends on the definition of the input parameters and must be verified using experimental data. Therefore, in this work the influence of process parameters as laser power and speed on the morphological and dimensional characteristics of melt pool was analysed for AISI 316L stainless steel single scan tracks. A commercial simulation software, FLOW-3D AM ®, was used for numerical modelling. The simulation results were experimentally verified so that model reliability was validated and input parameters optimized.

KEYWORDS: NUMERICAL SIMULATION, ADDITIVE MANUFACTURING, LASER POWDER BED FUSION (L-PBF), STAINLESS STEEL.

INTRODUCTION

Laser powder bed fusion (L-PBF) is an additive manufacturing (AM) technique that involves the melting of a powder layer by using a laser moving according to predefined paths [1]. The localized action of the laser, with an extremely high power, leads to the melt pools formation which, solidifying quickly, turn into tracks of solid material; then, the subsequent deposition of new layers of powder followed by corresponding laser passes allows the creation of the component in three dimensions, layer by layer. This technique promotes a great freedom of design, a limited need for machining operations, thus ensuring a minimum waste of material, together with remarkable mechanical properties. Despite these numerous advantages [2], the obtained components often show a level of defects that can present serious critical issues for their service life. Furthermore, the ability to monitor the process in real time is very difficult, given the high speed and complexity of the physical phenomena taking place at melt pool scale [3]. Therefore, a successful numerical simulation software for AM technologies would represent a valid tool to control the evolution of the process, predict the presence of defects and evaluate the influence of the various parameters on the final quality.

M. B. Abrami, C. Ransenigo, M.Tocci, A. Pola, M. Obeidi, D. Brabazon
Dipartimento di Ingegneria Meccanica e Industriale, Università degli Studi di Brescia, Via Branze 38, 25123, Brescia, Italia - Corresponding author: Maria Beatrice Abrami - m.abrami003@unibs.it

Muhannad Obeidi, Dermot Brabazon
I-Form, Advanced Manufacturing Research Centre, School of Mechanical and Manufacturing Engineering, Dublin City University, Glasnevin, Ireland

In this regard, some studies investigated the effectiveness of simulation software for the defects prediction: for example, Lee et al. [4] analysed the influence of laser power and speed on the arising of balling defect, i.e. surface protrusions, while Khairallah et al. [5] identified which laser properties have the greatest influence on the spatter, drops of liquid expelled and deposited on the already processed areas.
Instead, other researches exploited the potential of simulation software with the aim of optimizing process parameters, in particular by referring to the analysis of the morphology of the single scan tracks, as the minimum unit that constitutes additive manufactured parts [6].
Various authors have used this method also in experimental studies in order to define the optimum process parameters based on morphology and size of the scan tracks [7-9]. Indeed, several deposition parameters can affect the final quality of the fabricated parts [10], among which laser power, scanning speed, particle size distribution (PSD) and powder bed thickness play a major role in determining microstructural and mechanical properties. Therefore, producing single scan track varying one-by-one the process parameters appears particularly useful since it is possible to study their effect on a small portion of material.
As for any other manufacturing simulation software, it is fundamental to define appropriately all the input pre-processing parameters in order to model the real process in a reliable way. However, some of them are not uniquely defined or easily available yet, which makes the AM simulation a powerful but not fully validated tool and thus further investigations are needed.
Therefore, in this work the commercial software FLOW-3D AM was used to investigate the influence of some process parameters (laser power, laser speed, layer thickness) on simulations of single scan tracks, and the prediction reliability was verified by manufacturing samples in AISI 316L stainless steel. Among the various alloys studied for additive manufacturing applications, AISI 316L stainless steel represents an interesting material for its engineering applications in a wide range of fields (medical devices, food processing, pharmaceutical, aerospace and marine components) [11, 12]. Furthermore, it can be successfully processed by laser powder-bed fusion process as demonstrated by a number of studies [13-16]. However, the physical phenomena taking place during the process are extremely complex and the formation of defects, such as porosities or solidification cracks, is often reported [17, 18]. In general, the definition of a general approach to produce sound parts with high mechanical properties is still an open question. Therefore, AISI316L steel appears a suitable material for the present study.
The experimental validation of the model allowed to verify the validity of input parameters and the reliability of the numerical model. This is relevant to propose a sound approach to study the effects of process parameters by numerical modelling. This is time and cost-saving and allows a more effective analysis as opposed to a trial and error approach during the first steps of production.

EXPERIMENTAL PROCEDURE

NUMERICAL MODEL

Simulation of L-PBF process with AISI 316L stainless steel powders was the object of the study. Simulations were carried out by using the commercial software FLOW-3D AM, which consists in two modules. First, the powder bed generation was modelled using DEM (Discrete Element Method), while the melting of the powder when hit by the laser and the following melt pool solidification was simulated using the WELD module (Finite Volume Method, FVM).
DEM requires as input parameters the particle size distribution and the friction coefficients with the walls and among the powder particles themselves, considered as rigid spheres. In this way, it is possible to model the relative movement of the particles when hit by the blade and spread over a substrate to form the powder bed. The PSD used as simulation input for the case studies discussed in the present work was extracted from [19], where it was measured with laser diffraction technique, and approximated with discrete intervals, as reported in Fig.1 .

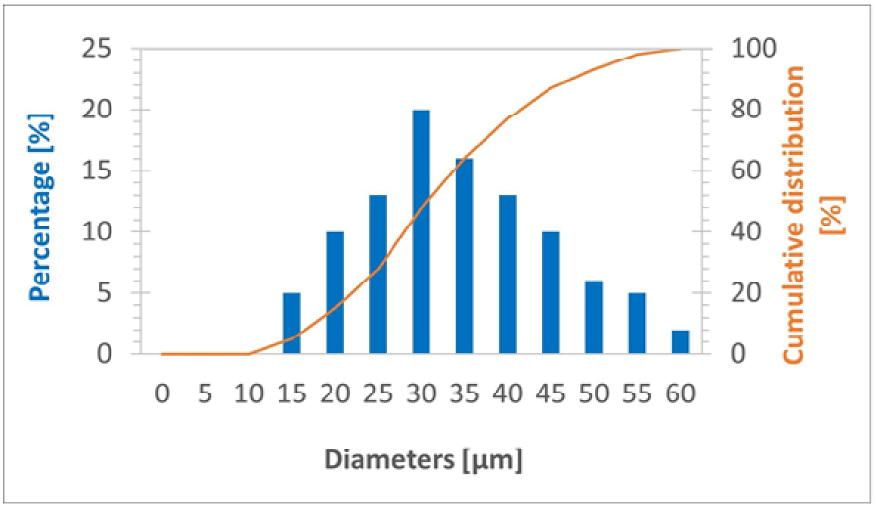

Fig.1 Particle size distribution of powders

Once the layer is obtained, it is converted into a .stl file and imported into the WELD module in which, after setting the process parameters, the simulation of the melting and solidification phase can be performed. Process parameters related to the different cases studies are presented in Tab.1.

Tab.1 - Simulation parameters of the cases of study.

Track	Power [W]	Scanning speed [cm/s]	Layer thickness [µm]
A	140	50	60
B	140	100	60
C	140	50	60
D	140	100	60
E	140	50	90
F	140	100	90
G	140	50	90
H	140	100	90

Simulations were carried out with different combinations of laser power and speed to study their effects on the quality and morphology of the track obtained. The four combinations presented in Tab.1 were then repeated for the case of layer thickness of 60 µm and of 90 µm. A mesh of about 1.2 million of elements was created for each case. Finally, to set simulations it is necessary to define the parameter called "Fluid Absorption Rate" which quantifies the laser energy absorbed by the substrate. A value of 0,6 was used as suggested by the literature [20]. Concerning the laser spot size, it was set equal to 36 µm.

From the elaboration of the simulation results, it was possible to perform measurements of melt pool dimensions, which were then used for the model validation by comparison with data obtained from experimental tests. In addition, the morphology of the simulated tracks was compared with the real track (details in the next paragraph).

For the cases showing a good match with experimental results, melt pool dimensions were measured in six different sections. Based on the measurements obtained from simulations, the melt pool depth/width ratio was calculated to investigate the melting mode. Indeed, there are two different melting modes determining distinct depth profiles and melt pool shapes. Keyhole melting mode happens when temperature in the melt pool is too high above the liquidus temperature and consequently metal vaporization can occur causing voids formation. The strong recoil pressure generated as result creates a deep melt pool with a keyhole shape and a high depth-to-width ratio. If the maximum temperature is lower than the boiling one, a conduction melting mode regime can be detected, characterized by a roughly semi-cylindrical shape of the melt pool. The melting mode determination is necessary for the track stability evaluation, as keyhole mode is associated with a greater presence of defects (keyhole porosity, spatter), while the conduction mode involves greater stability and process control and as such is the desired one [21].

EXPERIMENTAL ANALYSIS

The alloy used in the present study is commercial AISI 316L stainless steel powder. Details on chemical composition can be found in [19]. Samples were manufactured as single scan tracks of 10 mm length. The samples were produced in an Aconity Mini building chamber saturated with Ar, using the same parameters reported in Tab.1. The laser spot size was 36 μm.

First, the top view of the tracks was analysed with LEICA DMS 300 digital microscope to observe the track morphology. Then the scan tracks were cut, mounted in acrylic resin and polished up to mirror finishing. The obtained samples were etched in Vilella reagent in order to highlight the presence of melt pools and the microstructure and observed with LEICA DMI5000M optical microscope.

RESULTS

TRACK MORPHOLOGY EVALUATION

Fig. 2 shows the comparison between simulated and real tracks in order to observe their morphology as a function of the different process parameters tested for the layer with thickness of 60 μm. Analogously, Fig. 3 shows the same comparison for a layer of thickness of 90 μm.
From this comparison, three main cases appear: 1) good agreement between results (simulations A, B, E, F) when the morphology of the real track is well predicted by the simulation; 2) partial agreement between results (simulations C, G) when the track morphology is well modelled only in the second half; 3) no agreement between results (simulation D, H).

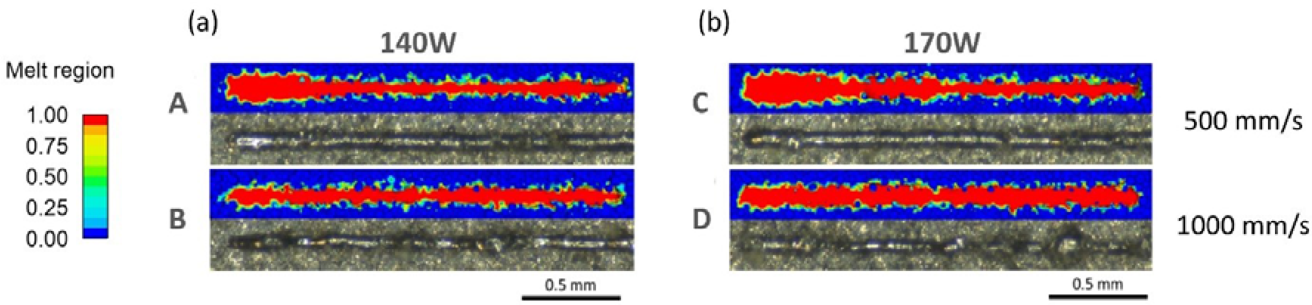

Fig.2 Comparison between simulation and experimental results of track morphology, with 60 μm of layer thickness and with (a) 140 W and (b) 170 W of laser power, see Table 1 for further process parameters.

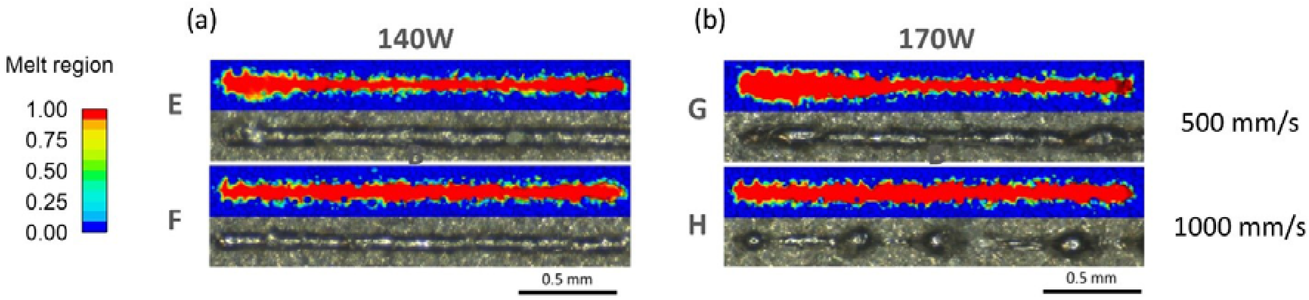

Fig.3 Comparison between simulation and experimental results of track morphology, with 90 μm of layer thickness and with (a) 140 W and (b) 170 W of laser power, see Table 1 for further process parameters.

From these comparisons, it emerges that as laser speed increases, real track morphologies are not well predicted by the software. This is due to the wide window of simulation parameters combination used: in these conditions, it was noted that the parameter "Fluid Absorption Rate" depends on laser power and speed. This result appears extremely relevant since in literature, "Fluid Absorption Rate" is usually set as constant and its dependence on the process parameters is not normally taken into consideration. In fact, the "Fluid Absorption Rate" parameter can be correlated to the physical property of absorptivity [20], which represents the fraction of incident radiation absorbed or absorbable by the body, in this case by the powder bed. This property varies significantly depending on many factors, such as the material surface roughness, PSD, spatial distribution of particles, laser beam size, and on laser power and velocity. This confirms the need to fully understand how to set the "Fluid Absorption Rate" parameter within simulations in order to obtain reliable results able to predict reality.

Another dependence to take in consideration is that of temperature, in particular for the modelling of the initial part of the track, which in some cases (i.e. Fig.2b-3b) appears too wide compared to reality. In fact, this area is characterized by high overheating due to the laser turn on, especially when the power is high. Therefore, in this regard, setting a "Fluid Absorption Rate" depending on temperature could provide more precise simulation results. Finally, the last aspect to be considered concerns the volume of metal surrounding the track: in the model, the simulated metal surface is in fact much smaller (3 x 0.5 mm) than that of the real process. For this reason, in simulations, heat exchange is limited and the heat retained by the powder and melted metal is greater. Simulating a larger surface of powders and substrate would better represent the real process conditions and should allow more reliable results to be obtained.

MELT POOL DIMENSIONS

Further analyses were carried out for the tracks characterized by good agreement between simulations and experimental evidence, i.e. tracks A, B, C, E, F, G. The size of the melt pool was measured for these tracks in terms of width, length, and height, as shown in Fig.4.

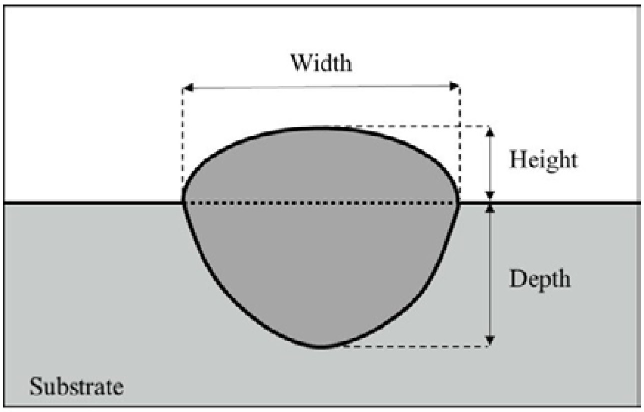

Fig.4 Schematic representation of size measurements for the cross section of melt pool.

Measurements were repeated in six different sections for each sample and average value and standard deviations were calculated. For the simulated tracks showing partial agreement, measurements were performed only in the second half of the scan, which was the most in line with the experimental track. Results are summarized in Fig. 5. It can be noted that as laser scanning speed increases, melt pool width and depth decreases due to the lower energy provided to the powder bed. Conversely, by increasing power, dimensions increase due to the greater molten volume of powders. Similar relative variations were predicted from the simulations in melt pool width, depth and height.

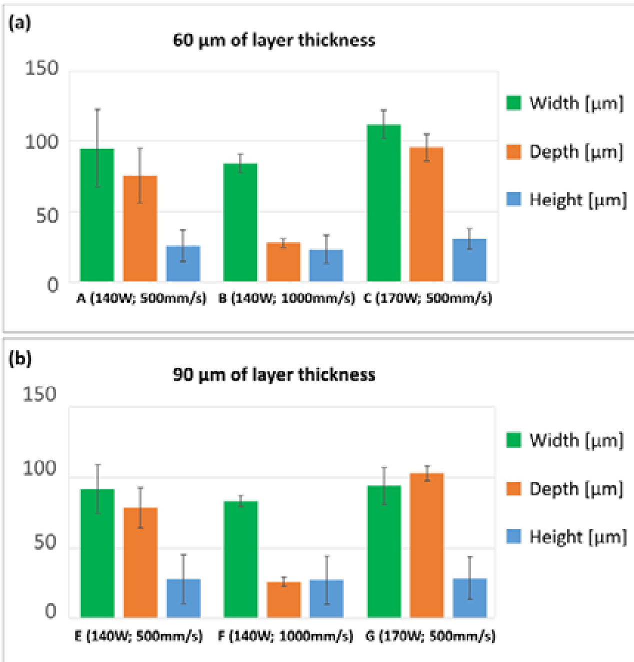

Fig.5 Melt pool measures (and corresponding standard deviation) for simulated tracks in agreement with real tracks, in the cases of a layer thickness of (a) 60 μm and (b) 90 μm

Based on numerical simulation results, the depth/width ratio was also calculated, shown in Fig. 6, with the aim to investigate the melting mode for each track.

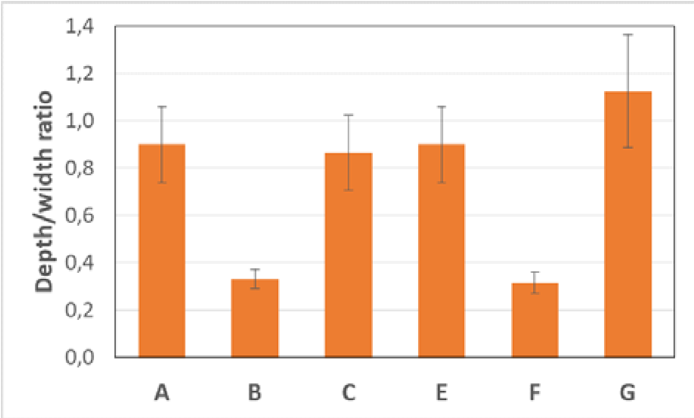

Fig.6 Depth/width ratio (and corresponding standard deviation) for simulated tracks in agreement with real tracks.

MODEL VALIDATION

Analysing values reported in Fig. 6, it emerges that the only sample likely exposed to a keyhole melting mode is track G, being the only one with average value of depth/width ratio slightly higher than 1. Tracks B and F exhibit instead the lowest depth/width ratio, and as such should ensure a stable conduction melting mode. To verify this, cross sections of these tracks were observed by optical microscope. Results of the comparisons are shown in Fig. 7, both in terms of melt pool morphology and dimension. It can be noticed that both the real melt pools are characterized by a semi-cylindrical shape, typical of the conduction mode, as predicted by simulations. Furthermore, dimensional analysis shows a good agreement between simulated and experimental results, thus confirming the validity of the model.

(a)

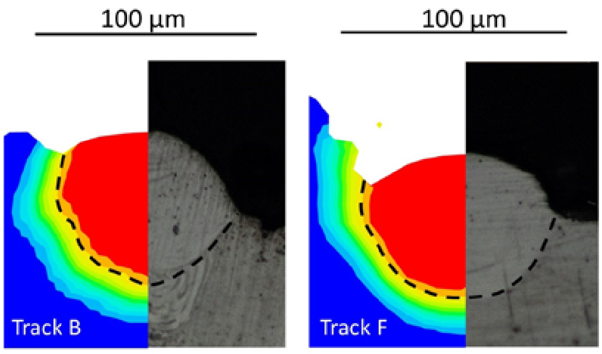

(b)

		Simulated measurements [µm]	Experimental measurements [µm]
Track B	Width	84 ± 6	76
	Depth	28 ± 3	27 (61)
	Height	23 ± 10	37
Track F	Width	83 ± 4	71
	Depth	26 ± 3	38
	Height	27 ± 17	25

Fig.7 Simulation and experimental results for track B and F, for (a) shape and (b) dimensions of the melt pool.

CONCLUSIONS

In the present work, numerical simulations of laser powder bed fusion of several single scan tracks in AISI 316L were carried out. Simulation results were then experimentally validated, in terms of morphology and dimensions of the tracks obtained. The case studies presented demonstrate the numerical simulation potentiality of effectively represent additive manufacturing processes. In particular, the need to properly calibrate the numerical modelling according to the process parameters was highlighted, as a key aspect to exploit the software potential in the best way. When this occurs, in fact, as investigated for the "Fluid Absorption Rate" parameter, the software prediction capability is extremely accurate. Despite the small size of geometries used in the simulations, results obtained are representative of larger samples, taking advantage of the stratified construction typical of additive manufacturing processes.

ACKNOWLEDGEMENTS

The authors would like to acknowledge Filippo Palo for technical support for FLOW 3D-AM. This study is supported by a research grant from Science Foundation Ireland under Grant Number 16/RC/3872 and co-funded under the European Regional Development Fund.

REFERENCES

[1] D. Gu, M. Xia, and D. Dai, "On the role of powder flow behavior in fluid thermodynamics and laser processability of Ni-based composites by selective laser melting," International Journal of Machine Tools and Manufacture, Article vol. 137, pp. 67-78, 2019, doi: 10.1016/j.ijmachtools.2018.10.006.

[2] G. C. Karar, R. Kumar, and S. Chattopadhyaya. An analysis on the advanced research in additive manufacturing, Lecture Notes in Mechanical Engineering, pp. 229-277, 2021.

[3] U. Scipioni Bertoli, G. Guss, S. Wu, M. J. Matthews, and J. M. Schoenung, "In-situ characterization of laser-powder interaction and cooling rates through high-speed imaging of powder bed fusion additive manufacturing," Materials and Design, Article vol. 135, pp. 385-396, 2017, doi: 10.1016/j.matdes.2017.09.044.

[4] Y. S. Lee and W. Zhang, "Mesoscopic simulation of heat transfer and fluid flow in laser powder bed additive manufacturing," in Proceedings - 26th Annual International Solid Freeform Fabrication Symposium - An Additive Manufacturing Conference, SFF 2015, 2020, pp. 1154-1165. [Online]. Available: https://www.scopus.com/inward/record.uri?eid=2-s2.0-85084931105&partnerID=40&md5=259f005dd1dfff5358b095f470519fc2

[5] S. A. Khairallah et al., "Controlling interdependent meso-nanosecond dynamics and defect generation in metal 3D printing," Science, Article vol. 368, no. 6491, pp. 660-665, 2020, doi: 10.1126/science.aay7830.

[6] Y. C. Wu, W. S. Hwang, C. H. San, C. H. Chang, and H. J. Lin, "Parametric study of surface morphology for selective laser melting on Ti6Al4V powder bed with numerical and experimental methods," International Journal of Material Forming, Article vol. 11, no. 6, pp. 807-813, 2018, doi: 10.1007/s12289-017-1391-2.

[7] A. Aversa et al., "Single scan track analyses on aluminium based powders," Journal of Materials Processing Technology, vol. 255, pp. 17-25, 2018/05/01/ 2018, doi: https://doi.org/10.1016/j.jmatprotec.2017.11.055.

[8] U. Scipioni Bertoli, A. J. Wolfer, M. J. Matthews, J.-P. R. Delplanque, and J. M. Schoenung, "On the limitations of Volumetric Energy Density as a design parameter for Selective Laser Melting," Materials & Design, vol. 113, pp. 331-340, 2017/01/05/ 2017, doi: https://doi.org/10.1016/j.matdes.2016.10.037.

[9] A. S. Sabau et al., "Fluid Dynamics Effects on Microstructure Prediction in Single-Laser Tracks for Additive Manufacturing of IN625," Metallurgical and Materials Transactions B: Process Metallurgy and Materials Processing Science, Article vol. 51, no. 3, pp. 1263-1281, 2020, doi: 10.1007/s11663-020-01808-w.

[10] I. Yadroitsev, P. Bertrand, and I. Smurov, "Parametric analysis of the selective laser melting process," Applied Surface Science, vol. 253, no. 19, pp. 8064-8069, 2007/07/31/ 2007, doi: https://doi.org/10.1016/j.apsusc.2007.02.088.

[11] X. Niu et al., "Review of materials used in laser-aided additive manufacturing processes to produce metallic products," Frontiers of Mechanical Engineering, vol. 14, no. 3, pp. 282-298, 2019/09/01 2019, doi: 10.1007/s11465-019-0526-1.

[12] I. Tolosa, F. Garciandía, F. Zubiri, F. Zapirain, and A. Esnaola, "Study of mechanical properties of AISI 316 stainless steel processed by "selective laser melting", following different manufacturing strategies," The International Journal of Advanced Manufacturing Technology, vol. 51, no. 5, pp. 639-647, 2010/11/01 2010, doi: 10.1007/s00170-010-2631-5.

[13] D. Wang, C. Song, Y. Yang, and Y. Bai, "Investigation of crystal growth mechanism during selective laser melting and mechanical property characterization of 316L stainless steel parts," Materials & Design, vol. 100, pp. 291-299, 2016/06/15/ 2016, doi: https://doi.org/10.1016/j.matdes.2016.03.111.

[14] D.-R. Eo, S.-H. Park, and J.-W. Cho, "Inclusion evolution in additive manufactured 316L stainless steel by laser metal deposition process," Materials & Design, vol. 155, pp. 212-219, 2018/10/05/ 2018, doi: https://doi.org/10.1016/j.matdes.2018.06.001.

[15] T. R. Smith, J. D. Sugar, C. San Marchi, and J. M. Schoenung, "Strengthening mechanisms in directed energy deposited austenitic stainless steel," Acta Materialia, vol. 164, pp. 728-740, 2019/02/01/ 2019, doi: https://doi.org/10.1016/j.actamat.2018.11.021.

[16] T. Larimian, M. Kannan, D. Grzesiak, B. AlMangour, and T. Borkar, "Effect of energy density and scanning strategy on densification, microstructure and mechanical properties of 316L stainless steel processed via selective laser melting," Materials Science and Engineering: A, vol. 770, p. 138455, 2020/01/07/ 2020, doi: https://doi.org/10.1016/j.msea.2019.138455.

[17] M. S. F. de Lima and S. Sankaré, "Microstructure and mechanical behavior of laser additive manufactured AISI 316 stainless steel stringers," Materials & Design, vol. 55, pp. 526-532, 2014/03/01/ 2014, doi: https://doi.org/10.1016/j.matdes.2013.10.016.

[18] Z. E. E. Tan, J. H. L. Pang, J. Kaminski, and H. Pepin, "Characterisation of porosity, density, and microstructure of directed energy deposited stainless steel AISI 316L," Additive Manufacturing, vol. 25, pp. 286-296, 2019/01/01/ 2019, doi: https://doi.org/10.1016/j.addma.2018.11.014.

[19] M. Ahmed Obeidi et al., "Comprehensive assessment of spatter material generated during selective laser melting of stainless steel," Materials Today Communications, Article vol. 25, 2020, Art no. 101294, doi: 10.1016/j.mtcomm.2020.101294.

[20] B. Cheng, L. Loeber, H. Willeck, U. Hartel, and C. Tuffile, "Computational Investigation of Melt Pool Process Dynamics and Pore Formation in Laser Powder Bed Fusion," Journal of Materials Engineering and Performance, Article vol. 28, no. 11, pp. 6565-6578, 2019, doi: 10.1007/s11665-019-04435-y.

[21] U. Scipioni Bertoli, A. J. Wolfer, M. J. Matthews, J. P. R. Delplanque, and J. M. Schoenung, "On the limitations of Volumetric Energy Density as a design parameter for Selective Laser Melting," Materials and Design, Article vol. 113, pp. 331-340, 2017, doi: 10.1016/j.matdes.2016.10.037.